21st Australasian Fluid Mechanics Conference
Adelaide, Australia
10-13 December 2018

Tilting of Vortex Rings in Cross-flow

E. R. Hassan and R. M. Kelso

School of Mechanical Engineering
University of Adelaide, Adelaide, South Australia 5005, Australia

Abstract

This paper describes observations and measurements of the effect of cross-flow on the vorticity field of laminar vortex rings ejected from a circular pipe using particle-image velocimetry (PIV). We estimate positive-core circulation on the upstream side of the vortex ring and a negative circulation on the other side. Two pipe geometries are considered; one where the pipe exit is flush with a flat wall and one where the pipe exit is elevated above the wall. Vortex ring tilting is observed for both geometries.

Observation of the circulation development of the vortex cores shows that the circulation growth rate of the positive (upstream) vortex core is always smaller in magnitude than that of the negative (downstream) core. This is due to interaction of the vortex ring with regions of flow containing negative vorticity at the pipe exit. In the flush-mounted case, this negative vorticity is contained in the laminar boundary layer that develops over the wall. In the elevated case a shear layer that forms over the top of the elevated pipe contributes negative vorticity to the flow. Observations of the evolving vorticity fields for both geometries show that the motion of the positive vortex core in the pipe-axial direction is impeded by the presence of the cross flow. This impediment is not observed for the negative core. This difference in the motion of the vortex-ring cores results in the tilting of the vortex ring.

Introduction

When a laminar vortex ring is ejected from a circular pipe into a perpendicular uniform cross-flow, it tilts. The tilting occurs in the counter-clockwise direction for a left to right cross-flow. The cause of this tilting has been the subject of discussion in recent times. Chang & Vakili [1] and Sau & Mahesh [7] claim that the tilting is due to the Magnus effect whereby antisymmetric lift forces are generated on the opposite sides of the vortex ring. Lim *et al.* [6] contests this, claiming that the tiliting may be caused by a resitribution of the ring vorticity during the vortex formation process.

In this study we investigate the formation and subsequent development of a single vortex ring generated with two distinct boundary conditions. The change in boundary condition is from a pipe exit which is flush with a flat wall, to a pipe exit which is elevated above the wall. From velocity measurements in the plane containing the axis of the vortex ring we obtain the vorticity and the circulation of principal structures in the developing flow field.

Apparatus

Experiments are conducted in a confined section of a closed-return water channel with a working section of 500 mm $\times$ 500 mm $\times$ 2000 mm. A vortex ring is generated by impulsively translating a piston within a cylinder for a short period with the ideal piston velocity being a square-wave function of time. A stepper motor driving a lead screw advances the piston in a controlled and repeatable manner.

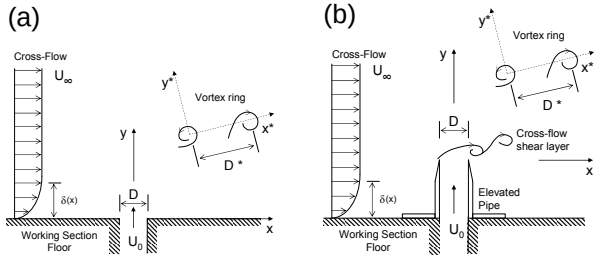

Figure 1: Configurations and coordinate systems of the (a) flush-mounted and (b) elevated geometries

Fluid from the cylinder flows through a hose into a pipe of diameter D=25 mm. The two pipe geometries considered are:

1. Flush-mounted: The exit plane of the pipe is flush mounted with the floor of the of the working section of the water channel.
2. Elevated: The pipe exit plane is 2.5D above the floor of the water channel and the outside of the pipe is tapered at an angle of 7^o to a sharp edge at the tip.

These geometries and related coordinate systems are shown schematically in figure 1.

PIV Method

Velocity components in the plane containing the axis of the pipe are measured by two-component Particle Image Velocimetry (2C-PIV). Details of the the PIV technique are identical to those presented in Hassan *et al.* [4]. Anomalous velocity vectors (outliers) are detected using a custom-built code which implements the universal median technique described by Westerweel and Scarano [8]. Detected outliers are replaced with a weighted average of valid surrounding vectors. For all results presented here, the number of outliers in any one velocity-vector field is less than 3% of the total number of vectors. An adaptive Gaussian window interpolator filters noise from the raw vector field. The flush and elevated cases were conducted at different times during a larger experimental campaign. As a result, there are differences in the sizes of PIV image region and resulting spatial resolution. The image regions are 93 mm $\times$ 93 mm and 126 mm $\times$ 126 mm for the flush and elevated geometries respecitvely.

Table 1 shows the size of the PIV image region and the number of times each flow was conducted for each of the geometric configurations. The velocity uncertainty, $(\delta_u/u_0)_{\max}$, is 11.5% and 8.1% for the flush and elevated cases respectively. This velocity uncertainty is evaluated for the worst-case conditions where the velocity gradient is largest. Elsewhere the error is significantly smaller.

A custom-built electronic controller synchronises the start of vortex generation with the next available laser pulse and enables the camera trigger. This ensures that the n-th PIV image pair in any one realisation is synchronised with the n-th image pair in all other realisations

Flush-mounted.				Elevated.			
U_∞ (mm/s)	$R = \frac{U_o}{U_\infty}$	$Re_\infty = \frac{U_\infty D}{\nu}$	No. of Realisations	U_∞(mm/s)	$R = \frac{U_o}{U_\infty}$	$Re_\infty = \frac{U_\infty D}{\nu}$	No. of Realisations
0	$\to \infty$	0	35	0	$\to \infty$	0	47
6.10	6.6	150	5	6.06	6.6	150	56
11.90	3.4	300	38	11.01	3.6	280	58
22.30	1.8	560	5	21.53	1.9	540	47

Table 1: Cross-flow velocities, Velocity ratios and the number of realisations of each flow.

Flow Conditions

The vortex ring flow conditions for flush and elevated vortex rings are identical. The vortex rings are generated by impulsively translating the piston within a cylinder for a duration of τ = 1 second. The spatially-averaged pipe exit velocity, $\overline{U(t)}$, is integrated over time to obtain the total length of the displaced fluid slug, $L_0 = \int_0^\infty \overline{U(t)}dt \approx 40$mm. The ratio of the displaced slug length to the duration of piston motion, $U_0 = L_0/\tau \approx 40$mm/s, is a vortex ring velocity scale. The period of piston motion corresponds to a nondimensional time of $\widetilde{t} = tU_0/D = 1.6$.

Four flow conditions are investigated, each at a different ratio of vortex ring velocity, U_o, to the cross-flow velocity, U_∞. The velocity ratio, $R = U_o/U_\infty$, is varied by changing the cross-flow velocity. Although care was taken to match cross-flow velocites between the two geometries, there are slight variations in these velocites. Table 1 describes the cross-flow velocities, velocity ratios and cross-flow Reynolds numbers (Re_∞) for the flush and elevated cases. Note that, without a cross flow, $R \to \infty$ and $Re_\infty = 0$. To ensure statistical reliability, data collection is repeated for each flow condition at each velocity ratio; Table 1 gives the exact numbers of realisations for each case.

Tests conducted with the crossflow in the absence of a vortex ring show that a Blasius boundary layer forms on the floor of the water channel. The boundary layer thickness is much smaller than the height of the elevated pipe. The cross flow interacts with the elevated pipe and forms a periodic vortex-shedding shear layer at the top of the pipe. Measurements are made of the circulation contained within the boundary layer and in the shear layer developed over the elevated pipe. These measurments indicate approximately contant negative values of both boundary layer and cross-flow shear layer circulations measured within the PIV image region.

Data Processing

The out-of-plane vorticity field, ω_z, of each time step of each realisation is estimated from the in-plane velocity components. The hybrid compact-Richardson extrapolation (CR4) vorticity-estimation scheme of Etebari & Vlachos [2] is a noise-optimised, fourth-order scheme which simultaneously reduces both the random error and the bias error. The total vorticity uncertainty, $(\delta_\omega/\omega_0)|_{\max}$, is 12.7% and 9.4% for the flush and elevated cases respectively. Vorticity is presented in the nondimensional form, $\widetilde{\omega}=\omega_z D/U_0$.

Circulation, Γ, of each vortex core is estimated by numerically integrating velocity components around the boundary of a region in which vorticity exceeds a threshold value. The total circulation uncertainty, $(\delta_\Gamma/\Gamma_0)|_{\max}$, is 5.4% and 4.6% for the flush and elevated cases respectively. Circulation is presented in the nondimensional form, $\widetilde{\Gamma}=\Gamma/(U_0 D)$.

Vorticity and circulation are estimated for each realisation and at each time step. Details of the methods and the associated error analysis are given in Hassan *et al.* [5].

Primary Features of the Vortex Ring in Cross Flow

In the absence of a cross flow ($R \to \infty$), a laminar vortex ring forms at the pipe exit for both the flush-mounted and elevated cases. Shortly after the piston stops, the vortex ring moves away along the axis of symmetry of the pipe. Observation of the evolving vorticity field shows two cross-sections of the vortex ring. One cross-section contains positive vorticity and is referred to as the positive core for convenience. The other cross-section contains negative vorticity and is referred to as the negative core. We define the centre of each vortex core as the location of the peak vorticity magnitude. The vortex cores remain equal in size and symmetric about the axis of the pipe. Further details of these vortex rings are availble in Hassan and Kelso [3].

The addition of a cross flow alters the generation and subsequent development of the vortex ring in both geometric configurations. With the flush mounted case, the vortex ring forms in the presence of the negative-vorticity boundary layer that develops along the water channel floor. In the elvevated case, the vortex ring interacts with the negative-vorticity cross-flow shear layer.

For both geometries, the votex ring tilts in the counter-clockwise direction, distorts, and convects in the direction of the cross-flow. The instantaneous nondimensional vorticity field at a nondimensional time of $\widetilde{t} = 4.8$ is shown in figure 2 for each geometry for similar values of the velocity ratio, R. The positive and negative vortex cores and the tilt angle, α, are clearly visible, as are some secondary flow features that develop between the vortex cores.

Vortex Ring Tilting

The tilt angle is measured from the transient near-field vorticty field data and is defined as the counterclockwise angle between the x-direction and the x^*-direction (a line joining the positive and negative vortex ring cores, centred at the positive core) as shown in figure 1. The ensemble average of the tilt angle across all realisations for each for each geometry and each velocity ratio is shown in figure 3. The tilt angle for the no cross-flow case ($R \to \infty$) is also shown for comparison and is zero as expected. The tilt angle increases with decreasing velocity ratio. The tilt angle for the flush-mounted cases increases steadily with time, whereas the tilt angle for the elevated cases exhibit a complicated behaviour with time. The elevated vortex rings pass through and interact with the cross flow shear layer that develops over the elevated pipe. This negative-vorticity shear layer is periodic in nature, whereas the vortex rings are generated without synchronising with any particular phase of shear-layer roll up. This may explain the varied nature of the tilt angle for the elevated cases.

The tilting comes about from a variation in the wall-normal position of the centre of each vortex core y_c (see figure 2). Figure 4 shows temporal development of y_c for the negative vortex core for both geometries. The wall-normal locations of the negative core in both cases are very similar with or without a cross flow.

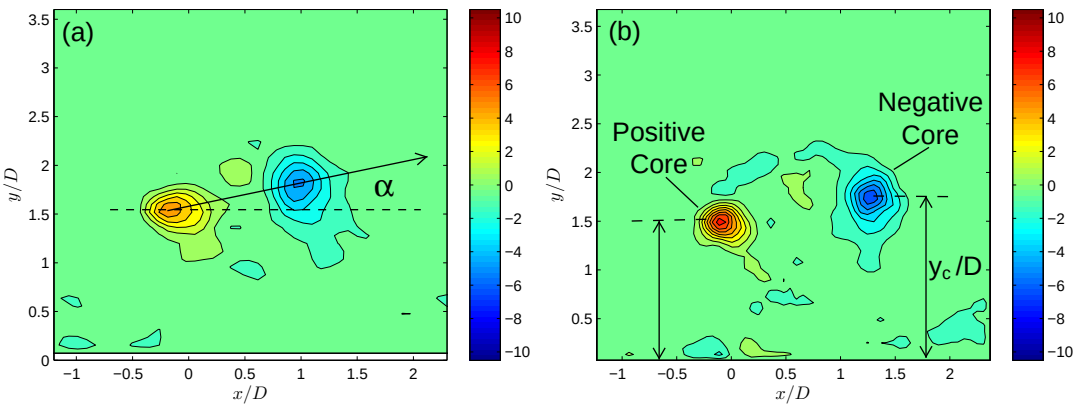

Figure 2: Nondimensional vorticity field, $\widetilde{\omega}$ of a vortex ring generated from a (a) flush-mounted ($R = 3.4$) and (b) elevated ($R = 3.6$) pipe at a nondimensional time of $\widetilde{t} = 4.8$. The cross-flow is from left to right.

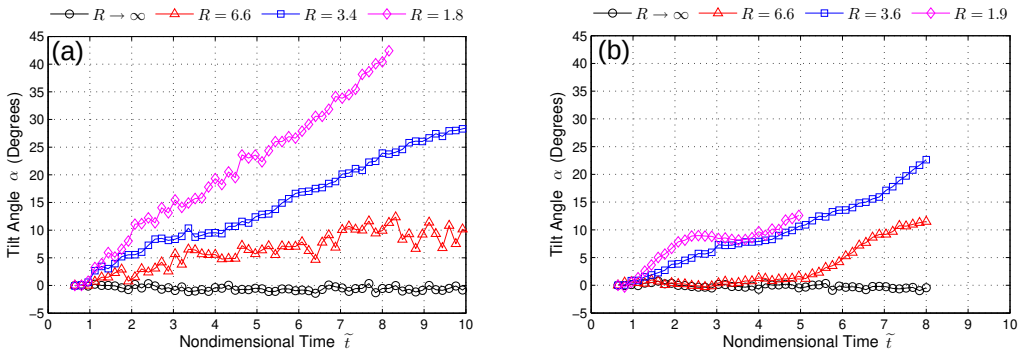

Figure 3: Ensemble-averaged tilt angle of vortex rings generated from (a) flush-mounted and (b) elevated geometries.

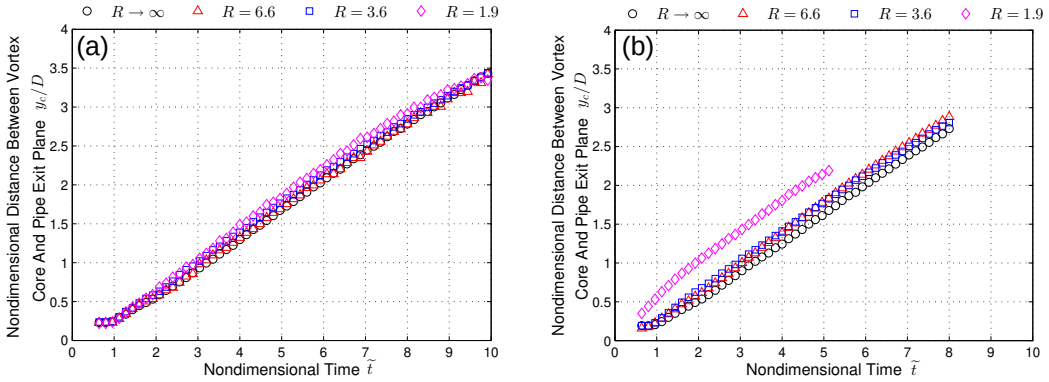

Figure 4: Development of the vertical distance between the negative vortex core and the pipe exit plane for the (a) flush-mounted and (b) elevated geometries.

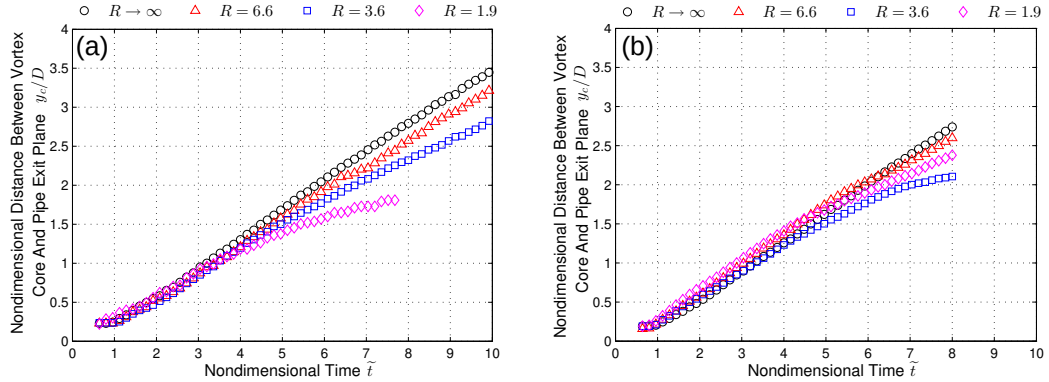

Figure 5: Development of the vertical distance between the positive vortex core and the pipe exit plane for the (a) flush-mounted and (b) elevated geometries.

This indicated that the cross flow has little effect on the wall-normal position of the negative core.

The positions of the positive cores, however, are significantly affected by the presence of the cross flow (figure 5). The flush case exhibits a clear reduction in the core wall-normal position with decreasing velocity ratio. This is due to the interaction with the steady negative-vorticity dominated boundary layer. This is verified by the fact that the rate of circulation growth of the positive vortex core is impeded by its interaction with the laminar boundary layer which is of opposite sign vorticity. This will be discussed in the next section. The positive vortex core position of the elevated cases are also reduced by the presence of the cross flow. The rate of circulation growth of the positive vortex core is impeded by its interaction with the cross-flow shear layer which is of opposite sign vorticity.

Circulation Growth

The temporal development of the ensemble-averaged circulation of each vortex core is shown in figure 6 for each geometry during the period of piston motion, $0 \lesssim \widetilde{t} \lesssim 1.6$. Positive values of circulation are measured for the positive cores and negative values for the negative cores. In the absence of a cross flow, the circulations increase almost linearly with time and are the same for the flush and elevated cases.

For both flush and elevated cases, the cross flow reduces the growth rate of positive vortex core circulation. This reduction increases with decreasing velocity ratio, R. This reduced circulation is due to vorticity cancellation between the positive core and negative vorticity in the boundary layer and the cross-flow shear layer for the flush and elevated cases respectively.

The rate of circulation growth of the negative core is unaffected by the cross flow for both geometries. Circulation is calculated by integrating the velocity around the boundary of a region in which vorticity exceeds a threshold. For the elevated case where the cross flow shear layer is developed at the pipe lip, the negative circulation in figure 6 b contains contributions from both the negative vortex core and the cross-flow shear layer. On the other hand, the calculation of positive circulation includes only the positive vortex core. The vertical offset from zero for the negative vortex cores in the elevated case correspond to the constant negative values of the cross-flow shear layer

For the flush mounted case, figure 6 a, some, but not all, of the negative-vorticity laden fluid within the boundary layer is ingested by the negative core during vortex ring formation. This additional negative vorticity, carried by the negative core as it passes through the boundary layer, results in the vertical offset from zero for the negative vortex cores in the flush case.

Conclusions

Measurements are made on the vorticity fields and circulations of laminar flush-mounted and elevated vortex rings. It is observed that:

1. Both flush and elevated vortex ring tilt when generated in the presence of a crossflow.
2. The circulation growth rates of the negative vortex cores is unaffected by the crossflow. Conversely, the circulation growth rates of the positive vortex cores are impeded by the the crossflow such that the circulation growth rates decrease with increasing crossflow velocities (decreasing velocity rario, R).
3. The vortex ring tilting is a result of impediment of the motion of the positive vortex core in the pipe-axial direction by the the cross flow. This impediment is not observed for the negative core.

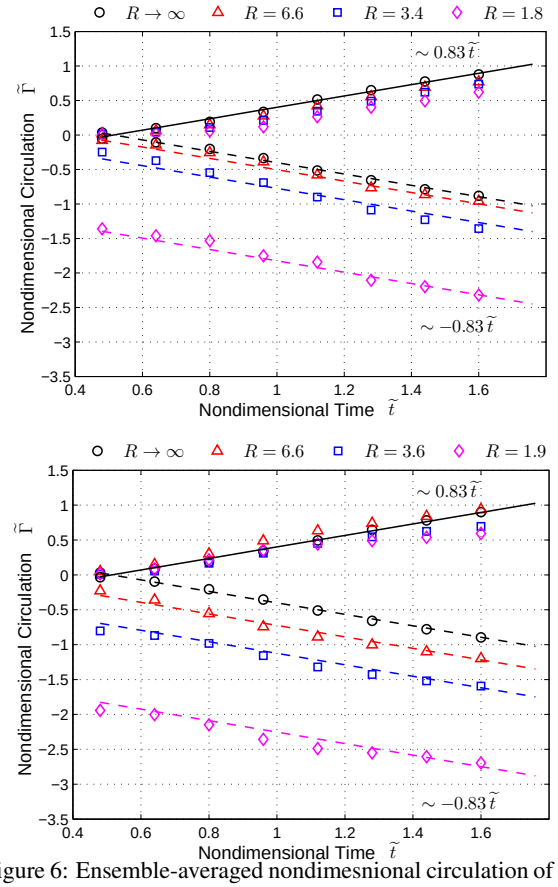

Figure 6: Ensemble-averaged nondimesnional circulation of the positive and negative vortex cores of a (a) flush and (b) elevated vortex ring in cross flow during vortex formation $0 \leq \widetilde{t} \leq 1.6$

References

[1] Chang, Y. and Vakili, A., Dynamics of vortex rings in cross-flow, *Physics of Fluids*, **7**, 1995, 1583–1597.

[2] Etebari, A. and Vlachos, P., Improvements on the accuracy of dervative estimation from dpiv velocity measurments., *Experiments in Fluids*, **39**, 2005, 1040–1050.

[3] Hassan, E. and Kelso, R., Vortex rings ejected from flush-mounted and elevated pipes, in *Proceedings of the* 21^{st} *Australasian Fluid Mechanics Conference, Adeladie, Australia*, The University of Adelaide, 2018.

[4] Hassan, E., Kelso, R. and Lanspeary, P. V., The effect of a uniform cross-flow on the circulation of vortex rings, in *Proceedings of the* 16^{th} *Australasian Fluid Mechanics Conference, Gold Coast, Australia*, The University of Queensland, 2007.

[5] Hassan, E., Lau, T. and Kelso, R., Accuracy of circulation estimation schemes applied to discretised velocity field data, in *Proceedings of the* 16^{th} *Australasian Fluid Mechanics Conference, Gold Coast, Australia*, The University of Queensland, 2007.

[6] Lim, T., Lua, K. and Thet, K., Does Kutta lift exist on a vortex ring in a uniform cross flow?, *Physics of Fluids*, **20**.

[7] Sau, R. and Mahesh, K., Dynamics and mixing of vortex rings in crossflow, *Journal of Fluid mechanics*, **604**, 2008, 389–409.

[8] Westerweel, J. and Scarano, F., Universal outlier detection for PIV data, *Experiments in Fluids*, **39**, 2005, 1096–1100.